

Quantum complementarity of microcavity polaritons

S. Savasta¹, O. Di Stefano¹, V. Savona², W. Langbein³

¹*Dipartimento di Fisica della Materia e Tecnologie Fisiche Avanzate,
Università di Messina, Salita Sperone 31, 98166 Messina, Italy*

²*Institut de Physique Théorique, Ecole Polytechnique Fédérale de Lausanne (EPFL), CH-1015 Lausanne, Switzerland*

³*Experimentelle Physik IIb, Universität Dortmund, Otto-Hahn-Str. 4, 44221 Dortmund, Germany*

(Dated: May 23, 2019)

We present an experiment that probes polariton quantum correlations by exploiting quantum complementarity. Specifically, we find that polaritons in two distinct idler-modes interfere if and only if they share the same signal-mode so that “which-way” information cannot be gathered. The experimental results prove the existence of polariton pair correlations that store the “which-way” information. This interpretation is confirmed by a theoretical analysis in terms of multi-particle quantum states.

PACS numbers: 71.36.+c, 42.50.Dv, 71.35.Gg, 42.50.Nn

Quantum complementarity is the essential feature distinguishing quantum from classical physics [1]. When two physical observables are complementary, the precise knowledge of one of them makes the other unpredictable. The most known manifestation of this principle is the property of quantum-mechanical entities to behave either as particles or as waves under different experimental conditions. Quantum complementarity is an inherent property of a quantum system, enforced by quantum correlations [1]. The link between quantum correlations, quantum nonlocality and Bohr’s complementarity principle was established in a series of “which-way” experiments using quantum-correlated photon pairs emitted via parametric down-conversion [2, 3, 4, 5]. We investigate this manifestation of quantum mechanics for cavity polaritons. Polaritons in semiconductor microcavities are hybrid quasiparticles consisting of a superposition of cavity photons and two-dimensional collective electronic excitations (excitons) in an embedded quantum well [6]. Owing to their mutual Coulomb interaction, pump polaritons generated by a resonant optical excitation can scatter into pairs of polaritons (signal and idler) according to total momentum and energy conservation [7, 8, 9, 10]. Polariton parametric emission has been recently observed [11, 12, 13]. In the low excitation limit it is a spontaneous process driven by vacuum-field fluctuations [9] whereas, already at moderate excitation intensity, it displays self-stimulation [12]. When instead an external probe beam is used to produce the final-state stimulation, the parametric scattering results in giant polariton amplification recently reported [14, 15, 16]. Parametric scattering is expected to produce multi-particle polariton states exhibiting quantum correlations [17].

In this letter we show evidence for quantum complementarity of cavity polaritons in a “which-way” experiment based on the polariton parametric process, in analogy with quantum-optics experiments [3, 4]. Our findings furthermore demonstrate the quantum pair-correlation of the emitted signal-idler polariton pairs. This fact, to-

gether with the possibility of ultrafast optical manipulation and ease of integration of these micro-devices, holds promise for applications in quantum information science.

The effective Hamiltonian describing the parametric polariton process is

$$\hat{H} = \sum_{\mathbf{k}} E_{\mathbf{k}} \hat{p}_{\mathbf{k}}^{\dagger} \hat{p}_{\mathbf{k}} + \sum_{\substack{\mathbf{k}, \mathbf{k}' \\ \mathbf{k}_s, \mathbf{k}_i}} \left[G(\mathbf{k}, \mathbf{k}') \hat{p}_{\mathbf{k}_s}^{\dagger} \hat{p}_{\mathbf{k}_i}^{\dagger} + \text{H.c.} \right] \delta_{\mathbf{k}_s + \mathbf{k}_i, \mathbf{k} + \mathbf{k}'}, \quad (1)$$

where the Bose operators $\hat{p}_{\mathbf{k}}^{\dagger}$ are the polariton creation operators, $E_{\mathbf{k}}$ is the polariton energy (Fig. 1a), and $G(\mathbf{k}, \mathbf{k}')$ contains details of the classical driving pump field and the polariton interaction. Given a pump wave vector \mathbf{k}_p , the final states of parametric processes satisfying energy and momentum conservation are represented by an “eight”-shaped curve in \mathbf{k} -space [7, 8], depicted in Fig. 1b. A pair of final states (signal and idler) is defined by the intersections of the curve with a straight line passing through \mathbf{k}_p . We denote as “idler” the modes with $k > k_p$. The experimental scheme that we devise employs two mutually coherent pump modes of momenta \mathbf{k}_{p1} and \mathbf{k}_{p2} with the classical amplitudes of the two pump-polariton fields $P_{\mathbf{k}_{p1}}$ and $P_{\mathbf{k}_{p2}}$, for which $G(\mathbf{k}, \mathbf{k}') = g P_{\mathbf{k}} P_{\mathbf{k}'} (\delta_{\mathbf{k}, \mathbf{k}_{p1}} + \delta_{\mathbf{k}, \mathbf{k}_{p2}}) (\delta_{\mathbf{k}', \mathbf{k}_{p1}} + \delta_{\mathbf{k}', \mathbf{k}_{p2}})$. The constant g is the polariton-polariton interaction amplitude, accounting for both the Coulomb interaction and the Pauli exclusion principle [15]. Two of the four products of δ ’s represent parametric processes driven by a single pump mode. The two other terms are mixed-pump processes involving one polariton from each pump mode, whose energy-momentum conservation defines the “peanut”-shaped curve illustrated in Fig. 1b (dashed). Let us first consider a pair produced by one pump only ($P_{\mathbf{k}_{p2}} = 0$). In the limit of low excitation intensity ($\tau = g |P_{\mathbf{k}_{p1}}|^2 t \ll 1$), the time evolution operator applied on the polariton vacuum state $|v\rangle$ yields the entangled polariton state $|\Psi\rangle = M |v\rangle_{s,i} + \tau |1\rangle_s |1\rangle_i$, where s and i label a pair of signal and idler modes on the “eight” (i.e. $2\mathbf{k}_{p1} = \mathbf{k}_s + \mathbf{k}_i$), and M is a normalization constant.

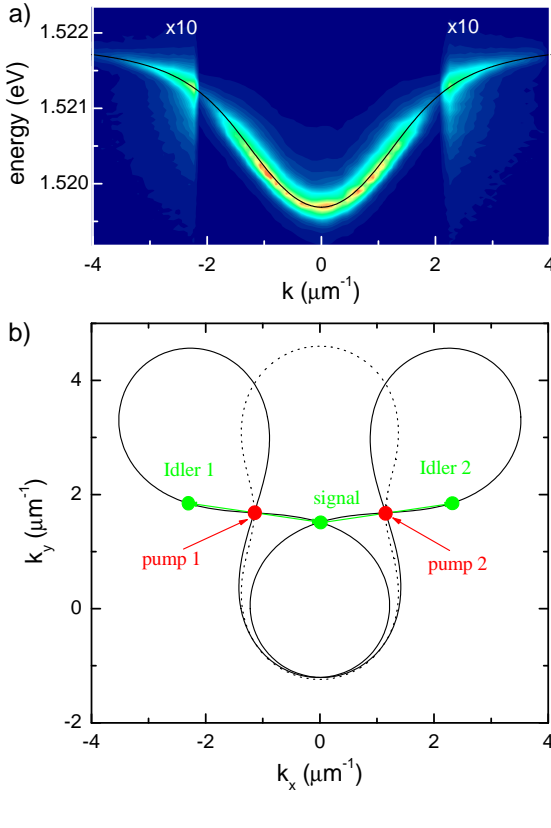


FIG. 1: Polariton dispersion and principle of the two-pump parametric processes. (a) Lower polariton photoluminescence intensity (linear color scale) as function of energy and $|\mathbf{k}|$. Excitation is in the upper polariton branch and the detuning between the cavity resonance and the energy of the heavy-hole exciton is -0.7 meV. The dispersion $E_{\mathbf{k}}$ (full line) calculated by means of a coupled-oscillator model [18] is superimposed. (b) \mathbf{k} -space plot of the final states fulfilling energy and momentum conservation in a two-pump parametric process. The two “eight”-shaped full curves represent the single-pump processes determined by the conditions $2\mathbf{k}_{pj} = \mathbf{k}_s + \mathbf{k}_i$ and $2E_{\mathbf{k}_{pj}} = E_{\mathbf{k}_s} + E_{\mathbf{k}_i}$, with $j = 1, 2$. The dotted line describes the mixed-pump process defined by $\mathbf{k}_{p1} + \mathbf{k}_{p2} = \mathbf{k}_s + \mathbf{k}_i$ and $E_{\mathbf{k}_{p1}} + E_{\mathbf{k}_{p2}} = E_{\mathbf{k}_s} + E_{\mathbf{k}_i}$. Two parametric processes sharing the same signal and thus giving rise to mutual idler coherence are also depicted.

This quantum state shows that the parametric process produces signal-idler pair correlations, i.e. that the scattered polaritons are created in signal-idler pairs. We now consider two mutually coherent pump polariton fields of equal amplitudes $P_{\mathbf{k}_{p2}} = P_{\mathbf{k}_{p1}} e^{i\phi}$. For this scheme, pairs of parametric processes sharing the signal mode are allowed, as schematically depicted in Fig. 1b. Such a pair of processes involves two idler modes $i1$ and $i2$ and one common signal mode s . In the limit of low excitation intensity, the time evolution operator applied on the polariton vacuum state yields in this case

$$|\Psi\rangle = M |v\rangle_{s,i1,i2} + \tau |1\rangle_s (|1\rangle_{i1}|0\rangle_{i2} + e^{-2i\phi} |0\rangle_{i1}|1\rangle_{i2}). \quad (2)$$

The resulting polariton density at the signal mode $\langle \Psi | \hat{p}_{\mathbf{k}_s}^\dagger \hat{p}_{\mathbf{k}_s} | \Psi \rangle$ is independent of ϕ . Interference is absent due to the orthogonality of the superimposed idler states $i1$ and $i2$ in the parentheses. This quantum superposition stores the “which-way” information, each term in the sum representing one possible idler path. Interference is also absent from either idler-polariton density. A different result is found for the mutual coherence of the two idler modes, which is observable in the sum of the two idler polariton fields. The resulting particle density is $\langle \Psi | (\hat{p}_{\mathbf{k}_{i1}}^\dagger + \hat{p}_{\mathbf{k}_{i2}}^\dagger)(\hat{p}_{\mathbf{k}_{i1}} + \hat{p}_{\mathbf{k}_{i2}}) | \Psi \rangle = 2\langle \Psi | \hat{p}_{\mathbf{k}_{i1}}^\dagger \hat{p}_{\mathbf{k}_{i1}} | \Psi \rangle [1 + \cos(2\phi)]$. In this case interference occurs because the two idler modes are pair-correlated with the same signal mode, and thus even by a signal-idler coincidence measurement, no “which-way” information could be retrieved. The more general many-polariton state produced by the two-pump parametric process beyond the low excitation intensity limit is

$$|\Psi\rangle = \sum_{n=0}^{\infty} \sum_{m=0}^n c_n(t) |\psi_m^n\rangle_s |m\rangle_{i1} |n-m\rangle_{i2}, \quad (3)$$

with $c_n(t) = (\tanh \sqrt{2}\tau)^n / (\cosh \sqrt{2}\tau)$, and

$$|\psi_m^n\rangle_s = \frac{1}{\sqrt{2^n}} \binom{n}{m}^{1/2} e^{-2i\phi(n-m)} |n\rangle_s. \quad (4)$$

A similar analysis performed on this state instead of (2) leads to the same conclusions.

Polaritons at a given \mathbf{k} can be observed by detecting the photons emitted at the same in-plane momentum [19], which carry the polariton amplitude and phase information. In the experiment we therefore measure the mutual interference of the two emitted idler fields indicated in Fig. 1b as a function of the relative pump phase ϕ . This is accomplished by detecting two superimposed \mathbf{k} -resolved images of the polariton emission, one of which is preliminarily mirrored around the $k_x = 0$ axis. The investigated sample [18] consists of a 25 nm GaAs/Al_{0.3}Ga_{0.7}As single quantum well placed in the center of a λ -cavity with AlAs/Al_{0.15}Ga_{0.85}As Bragg reflectors. The wide GaAs quantum well shows a negligible inhomogeneous broadening of the fundamental exciton, so that polariton modes have a small broadening also at large \mathbf{k} . The sample was held at a temperature of 5 K. The dispersion of the lower polariton branch was determined by photoluminescence spectra as function of $|\mathbf{k}|$ (see Fig. 1a). The two mutually coherent pump pulses of 1 ps Fourier-limited duration with an adjustable phase delay ϕ are created by splitting the exciting laser pulses (see Fig. 2), and are synchronously impinging on the microcavity with $\mathbf{k}_{p1} = (k_{px}, k_{py})$ and $\mathbf{k}_{p2} = (-k_{px}, k_{py})$. The emitted photon field $\mathcal{E}_{\mathbf{k}}$ of the MC is directed through an interferometer creating the superposition $\mathcal{E}_{\mathbf{k}} + \mathcal{E}_{\mathbf{k}'}$, where $\mathbf{k} = (k_x, k_y)$ and $\mathbf{k}' = (-k_x, k_y)$. Blocking one of the detection interfer-

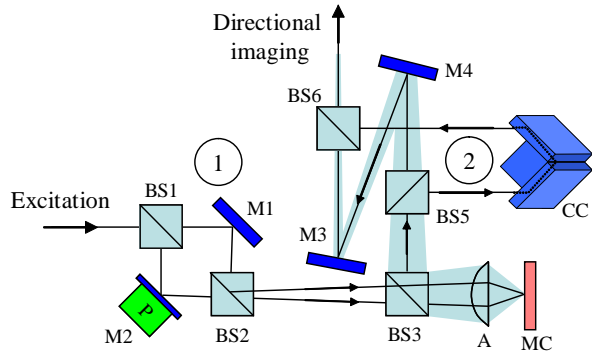


FIG. 2: Scheme of the optical setup used in the experiments. The excitation pulses were sent through a first Mach-Zender interferometer ① consisting of the mirrors M1, M2 and the beam-splitters BS1, BS2, in which the two phase coherent pump pulses are created. Their relative phase is adjustable by a piezoelectric element (P), and their individual directions can be adjusted by tilting the mirrors. The pump pulses are imaged by the aspheric lens A of 0.5 numerical aperture from the mirrors onto the microcavity. The emission from the microcavity is collected by the same lens, and directed by BS3 into a second Mach-Zender ② which, by using a double mirror (M3,M4) in one arm and a corner cube mirror (CC) in the other one, produces interference between fields at $\mathbf{k} = (k_x, k_y)$ and $\mathbf{k}' = (-k_x, k_y)$. The angular pattern of the outgoing intensity is detected. All beam-splitters are non-polarizing.

ometer arms, the intensity $I_{\mathbf{k}} = |\mathcal{E}_{\mathbf{k}}|^2$ is measured (see Fig. 3a), which is proportional to the polariton density $N_{\mathbf{k}} = \langle \Psi | \hat{p}_{\mathbf{k}}^\dagger \hat{p}_{\mathbf{k}} | \Psi \rangle$. We have modeled the parametric polariton emission originating from two pumps in terms of an extension of the density matrix formalism that was previously used in the single-pump case [7, 17]. This model shares the same physical assumptions as the simple quantum-state analysis presented here, but allows to obtain the \mathbf{k} -space dependence of the polariton density. It also accounts for an energy broadening mainly due to the photon escape rate out of the microcavity. The calculated polariton density (Fig. 3b) is in good qualitative agreement with the one deduced from the measured angular pattern of emission, thus supporting the assumption that the polariton parametric process dominates in the present experimental conditions. The quantitative deviations are attributed to a deformation of the polariton dispersion occurring at moderate polariton density [7].

Using both arms of the detection interferometer, the detected intensity $\tilde{I}_{\mathbf{k}} = |\mathcal{E}_{\mathbf{k}} + \mathcal{E}_{\mathbf{k}'}|^2$, proportional to the polariton density $\tilde{N}_{\mathbf{k}} = \langle \Psi | (\hat{p}_{\mathbf{k}}^\dagger + \hat{p}_{\mathbf{k}'}^\dagger)(\hat{p}_{\mathbf{k}} + \hat{p}_{\mathbf{k}'} | \Psi \rangle$, depends in general on the relative excitation phase ϕ of the pump pulses. To quantify the interference strength, we show in Fig. 4a the measured fringe visibility expressed as $V_{\mathbf{k}} = \sqrt{2[\langle (\tilde{I}_{\mathbf{k}})^2 \rangle_\phi / \langle \tilde{I}_{\mathbf{k}} \rangle_\phi^2 - 1]}$, where $\langle \dots \rangle_\phi$ denotes the average over ϕ . The experimental data show the appearance of interference, in qualitative agreement with the

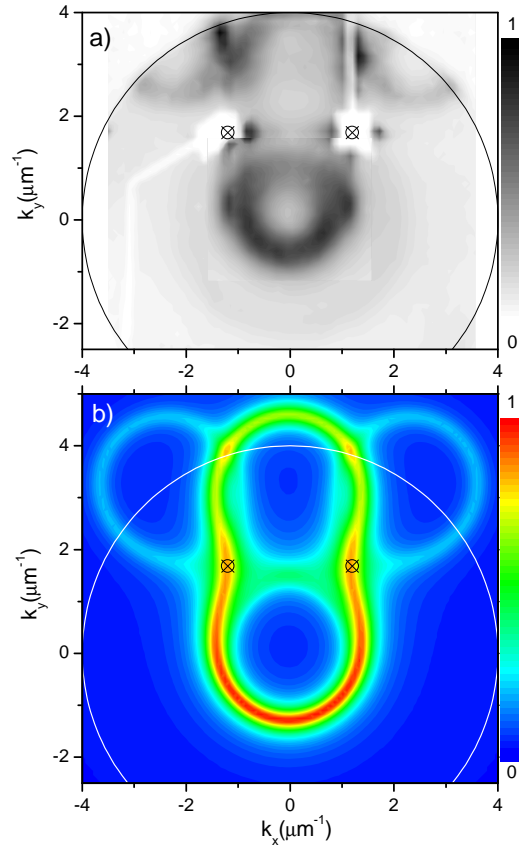


FIG. 3: Polariton density versus \mathbf{k} . The circles indicate the experimentally accessible \mathbf{k} -range, and the crosses the positions of the pump pulses. a) Measured for pulsed excitation of $\approx 9 \text{ nJ/cm}^2$, corresponding to an excited polariton density of $\approx 3 \times 10^9 \text{ cm}^{-2}$. The white shadows are masks blocking the pump beams. b) Simulated for cw-excitation using the experimentally determined polariton dispersion and pump momenta, and a constant polariton energy linewidth $\Gamma = 0.1 \text{ meV}$.

calculated visibility (Fig. 4b). To understand at which k_x the idler polaritons share the same signal mode, and thus interference is expected, we consider parametric processes driven by either one of the two pump modes. The pump at \mathbf{k}_{p1} produces the emission of polariton pairs at \mathbf{k} and $2\mathbf{k}_{p1} - \mathbf{k}$ respectively. Equivalently, the pump at \mathbf{k}_{p2} produces pairs of \mathbf{k}' and $2\mathbf{k}_{p2} - \mathbf{k}'$. By construction, the modes at $2\mathbf{k}_{p1} - \mathbf{k}$ and $2\mathbf{k}_{p2} - \mathbf{k}'$ have the same y-component but opposite x-components $\pm(2k_{px} - k_x)$. Consequently, idler modes at \mathbf{k} and \mathbf{k}' share the same signal mode if and only if $k_x = 2k_{px}$, at which also experimentally a finite visibility is observed (red in Fig. 4a). The ϕ -dependence of this interference (Fig. 4c) shows a $\cos(2\phi)$ behavior, as predicted by Eq. (2). The measured visibility vanishes when k_x departs from $2k_{px}$, i.e. when the idlers do not share the same signal mode (blue in Fig. 4a). Additionally, in agreement with the above quantum analysis, the signal at $k_x = 0$ displays no interference (dotted line in Fig. 4c) even though it is created by

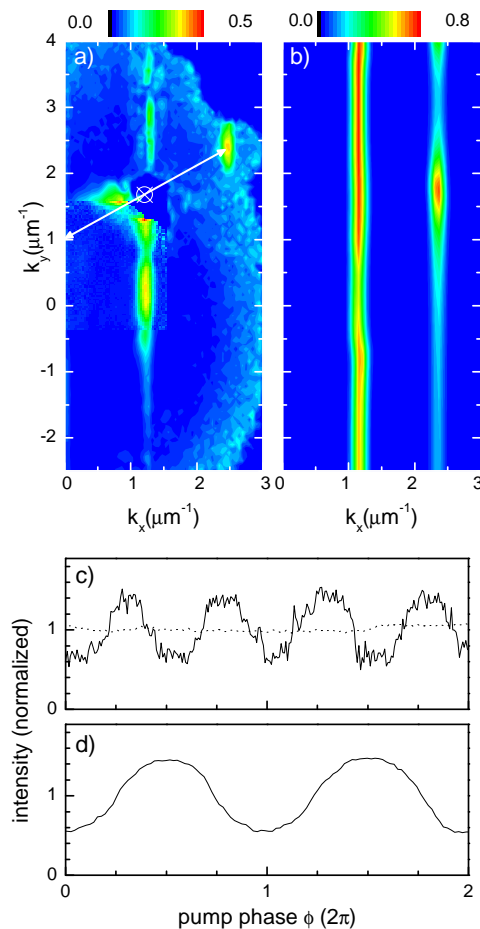


FIG. 4: Measured interference between parametric emission at \mathbf{k} and \mathbf{k}' . a) Measured interference visibility $V_{\mathbf{k}}$. The white arrows denote the parametric process sketched in Fig. 1b, for which the two idler-polaritons at $k_x = \pm 2k_{px}$ share the same signal-mode at $k_x = 0$. b) Simulated interference visibility. c) Measured intensity $\tilde{I}_{\mathbf{k}}$ at $\mathbf{k} = (2.4, 2.4)\mu\text{m}^{-1}$ (full) and at $\mathbf{k} = (0.0, 1.0)\mu\text{m}^{-1}$ (dotted) versus pump phase ϕ . d) Measured $\tilde{I}_{\mathbf{k}}$ at $\mathbf{k} = (1.2, 0.3)\mu\text{m}^{-1}$ versus pump phase ϕ .

a superposition of contributions from both pumps. The maximum of the measured visibility is about 0.5, as compared to 0.8 in the simulation. In the model, the visibility is reduced below one by the finite energy broadening, that allows non-resonant parametric processes not sharing the same signal-mode. In the experiment, the visibility is additionally reduced by scattering processes involving phonons or free charge carriers, producing uncorrelated light emission. The measured visibility is largely independent of the excitation density, being interference equally present both in the spontaneous and in the self-stimulated regime. In this latter, many-polariton entangled states [20, 21] are expected (Eq. 3). The visibility at $k_x = k_{px}$ is due to interference between two signal modes sharing the same idler mode and originating, respectively, from one of the two “eights” and from the

“peanut”-shaped mixed parametric process (see Fig. 1b). The “which-way” principle applies as in the previously discussed case. The measured interference (Fig. 4d) reveals a $\cos(\phi)$ -dependence, consistent with a generalization of the quantum-state analysis presented here. This interference mechanism has no analogy in the photon interference experiments employing two physically separate parametric downconverters [3, 4].

In conclusion, we have devised and performed an experiment where quantum-correlated states of electronic excitations (polaritons) in a semiconductor system were produced. We have observed polariton quantum complementarity enforced by polariton-pair quantum correlations. This result opens the possibility of producing many-particle entangled states of light-matter waves in a semiconductor, extending further the perspective of using solid-state micro-devices for the implementation of quantum information technology.

We are grateful to A. Callegari, B. Deveaud, R. Girlanda, A. Quattropani, P. Schwendimann, and R. Zimmermann for discussions and suggestions. W.L. acknowledges support by U. Woggon. The sample was grown by J.Riis Jensen at the Research Center COM and the Niels Bohr Institute, Copenhagen University. V. S. acknowledges funding from the Swiss National Science Foundation through project N. 620-066060.

- [1] M. O. Scully, B. G. Englert, H. Walther, *Nature* **351**, 111 (1991).
- [2] T. J. Herzog *et al.*, *Phys. Rev. Lett.* **75**, 3034 (1995).
- [3] X. Y. Zou, L. J. Wang, L. Mandel, *Phys. Rev. Lett.* **67**, 318 (1991).
- [4] L. Mandel, *Rev. Mod. Phys.* **71**, 274 (1999).
- [5] Y.-H. Kim *et al.*, *Phys. Rev. Lett.* **84**, 1 (2000).
- [6] C. Weisbuch *et al.*, *Phys. Rev. Lett.* **69**, 3314 (1992).
- [7] C. Ciuti, P. Schwendimann, A. Quattropani, *Phys. Rev. B* **63**, 041303R (2001).
- [8] W. Langbein, *Phys. Rev. B* **63**, to be published (2004).
- [9] S. Savasta, R. Girlanda, *Phys. Rev. Lett.* **77**, 4736 (1996).
- [10] S. Savasta, O. Di Stefano, R. Girlanda, *Phys. Rev. Lett.* **90**, 096403 (2003).
- [11] R. Houdré *et al.*, *Phys. Rev. Lett.* **85**, 2793–2796 (2000).
- [12] R. M. Stevenson *et al.*, *Phys. Rev. Lett.* **85**, 3680 (2000).
- [13] J. Erland *et al.*, *Phys. Rev. Lett.* **86**, 5791 (2001).
- [14] P. G. Savvidis *et al.*, *Phys. Rev. Lett.* **84**, 1547 (2000).
- [15] C. Ciuti, P. Schwendimann, B. Deveaud, A. Quattropani, *Phys. Rev. B* **62**, R4825 (2000).
- [16] M. Saba *et al.*, *Nature* **414**, 731 (2002).
- [17] P. Schwendimann, C. Ciuti, A. Quattropani, *Phys. Rev. B* **68**, 165324 (2003).
- [18] J. R. Jensen *et al.*, *Appl. Phys. Lett.* **76**, 3262 (2000).
- [19] V. Savona *et al.*, *Phys. Rev. B* **53**, 13051 (1996).
- [20] A. Lamas-Linares, J. C. Howell, D. Bouwmeester, *Nature* **412**, 887–890 (2001).
- [21] C. Simon, D. Bouwmeester, *Phys. Rev. Lett.* **91**, 053601 (2003).
- [22] D. S. Chemla, J. Shah, *Nature* **411**, 549 (2001).